

This article was downloaded by:

On: 23 January 2011

Access details: *Access Details: Free Access*

Publisher *Taylor & Francis*

Informa Ltd Registered in England and Wales Registered Number: 1072954 Registered office: Mortimer House, 37-41 Mortimer Street, London W1T 3JH, UK



## Journal of Liquid Chromatography & Related Technologies

Publication details, including instructions for authors and subscription information:

<http://www.informaworld.com/smpp/title~content=t713597273>

### The Fractal Approach to Secondary Mechanisms in SEC

R. García-Lopera<sup>a</sup>; Juan E. Figueruelo<sup>a</sup>; Iolanda Porcar<sup>a</sup>; Agustín Campos<sup>a</sup>; Concepción Abad<sup>b</sup>

<sup>a</sup> Departament de Química Física, Institut de Ciència dels Materials (ICMUV), Universitat de València, València, Spain <sup>b</sup> Departament de Bioquímica i Biologia Molecular, Universitat de València, València, Spain

**To cite this Article** García-Lopera, R. , Figueruelo, Juan E. , Porcar, Iolanda , Campos, Agustín and Abad, Concepción(2007) 'The Fractal Approach to Secondary Mechanisms in SEC', Journal of Liquid Chromatography & Related Technologies, 30: 9, 1227 – 1249

**To link to this Article:** DOI: 10.1080/10826070701274411

**URL:** <http://dx.doi.org/10.1080/10826070701274411>

PLEASE SCROLL DOWN FOR ARTICLE

Full terms and conditions of use: <http://www.informaworld.com/terms-and-conditions-of-access.pdf>

This article may be used for research, teaching and private study purposes. Any substantial or systematic reproduction, re-distribution, re-selling, loan or sub-licensing, systematic supply or distribution in any form to anyone is expressly forbidden.

The publisher does not give any warranty express or implied or make any representation that the contents will be complete or accurate or up to date. The accuracy of any instructions, formulae and drug doses should be independently verified with primary sources. The publisher shall not be liable for any loss, actions, claims, proceedings, demand or costs or damages whatsoever or howsoever caused arising directly or indirectly in connection with or arising out of the use of this material.

## The Fractal Approach to Secondary Mechanisms in SEC

**R. García-Lopera, Juan E. Figueruelo, Iolanda Porcar, and Agustín Campos**

Departament de Química Física and Institut de Ciència dels Materials (ICMUV), Universitat de València, València, Spain

**Concepción Abad**

Departament de Bioquímica i Biologia Molecular, Universitat de València, València, Spain

**Abstract:** Size-exclusion chromatography (SEC) is one of the most used experimental techniques to characterize polymers in solution; it has been applied to interpret the elution behaviour of many polymer-solvent systems in five types of column packings. The experimental data have revealed that the classical universal calibration is not accomplished. Deviations from a unique curve are a consequence of two effects: entropic (exclusion by size) and enthalpic (binary and ternary interactions between solvent, polymer, and gel), which results in secondary mechanisms accompanying the main “ideal” SEC separation mechanism. Therefore, three approaches of building a calibration curve have been compared in this work: (i) the classical universal calibration based on the elution of tetrahydrofuran (THF)-polystyrene (PS) system as reference; (ii) the specific or proper calibration curve made with standards of the sample under study; and (iii) the fractal calibration. The understanding of the secondary mechanisms has been based on the fractal characteristics of the porous gel surfaces, as well as on the swelling and cross-linking degrees. The global analysis of data has allowed us to propose an alternative relationship between the fractal dimension,  $D_f$ , and the chromatographic distribution coefficient,  $K_D$ , independently of the chemical nature of the solvent, polymer, and gel. From a quantitative point of view, the fractal methodology considerably reduces the deviations found when estimating polymer molar masses by SEC.

**Keywords:** Size-exclusion chromatography (SEC); Universal calibration; Fractal calibration

Address correspondence to R. García-Lopera, Departament de Química Física and Institut de Ciència dels Materials (ICMUV), Universitat de València, E-46100 Burjassot, València, Spain. E-mail: rosa.garcia@uv.es

## INTRODUCTION

Size-exclusion chromatography (SEC) is a separation technique in which different analytes can be resolved based on their molecular sizes in a solution. It is widely used to determine molar masses and distributions of synthetic polymers<sup>[1–6]</sup> and biomacromolecules.<sup>[7–9]</sup> In conventional SEC, calibration curves are commonly constructed by measuring the retention volumes (or retention times) of synthetic polymer standards with narrow molar mass distributions<sup>[3–5,10–12]</sup> and of monodisperse polymers in the case of biopolymers.<sup>[12,13]</sup> The subsequent transformation of the chromatographic peak into a molar mass distribution (MMD) allows the determination of the characteristic parameters: the weight-average molar mass ( $M_w$ ), number-average molar mass ( $M_n$ ), and polydispersity index ( $I$ ).

When separation of macromolecules is exclusively governed by size exclusion (“ideal” SEC), universal column calibration with polystyrene (PS) standards is normally used<sup>[1,14–18]</sup> and is valid if enthalpic contributions during the chromatographic separation are negligible.<sup>[9]</sup> However, generally, the commercially available SEC columns involve other mechanisms not exclusively related to size, such as adsorption or partition (or both) due to binary interactions between solvent, polymer solutes, and gel packing.<sup>[19–24]</sup> In fact, deviations from the universal calibration curve, at a given temperature, are observed for different polymer systems in a given gel packing, or even for the same system when eluting in different commercial chromatographic supports.<sup>[14,15,21,23,25–32]</sup> In all these situations, a specific (proper) calibration curve should be constructed for a given solvent-polymer-gel system, at constant temperature, based on standards of the same chemical nature as the polymeric sample under study. This fact implies that a set of well-characterized standards should be available for any putative polymeric sample. Obviously, this is not the real case, and the universal calibration with PS standards is generally used as reference in spite of the inherent errors committed in the determination of MMD and mass average parameters.

All probable interactions between solvent, polymer, and cross-linked gel can be simplified by considering the effect of the solute when it faces the gel as a rough surface. It is known that the porous gel material, used as packing in SEC, possesses a fractal geometry that can be characterized by means of the fractal dimension,  $D_f$ , which measures the roughness of the porous surface.<sup>[33–37]</sup> For organic packings,  $D_f$  depends both on the geometrical characteristics of the pore and on the heterogeneity of the porous surface,<sup>[38]</sup> leading to a strong enhancement of polymer-surface interactions, such as reversible adsorption, when the surface irregularity increases.<sup>[39]</sup> In this sense, there have been, recently, some attempts to mathematically model the separation of polymers in porous particles when both SEC and hydrodynamic chromatography (HDC) modes are present in the retention mechanism.<sup>[40]</sup> Moreover, another approach has shown the fractal properties of some alumino-silicate supports for metal catalysts by means of the SEC technique.<sup>[41]</sup>

In this work a relationship is shown between the fractal dimension of the pore surface and the chromatographic global distribution coefficient,  $K_D$ , which seems to be independent of the chemical nature of the solvent, polymer, and gel involved in the chromatographic system. The proposed fractal calibration (FC) has been proven to work well, at least when size-exclusion is the main separation mechanism and adsorption a secondary one. The usefulness of the FC is also demonstrated by comparing the values of the molar masses estimated from this approach with those deduced from the specific calibration curves, as well as from the tetrahydrofuran (THF)-PS calibration curve, as representative of the so-called universal calibration. All of them have been applied to polymer systems eluted in pure solvents or/and solvent mixtures, using pure gel packings or/and packing mixtures. We observe that the deviations in molar mass determination obtained with the FC are very similar to those deduced with the specific (proper) calibration curves, whereas important deviations appeared when using the THF-PS as reference. Thus, FC emerges as a suitable procedure to characterize polymer samples by SEC in order to determine  $M_w$ ,  $M_n$ , and  $I$ , especially when secondary effects (a very common event) are involved in the chromatographic separation process.

## THEORY

The main problem to deal with when characterizing an unknown polymeric sample by means of SEC in terms of  $M_w$ ,  $M_n$ , and  $I$ , consists of having a reliable and trusted calibration curve. Three procedures can be considered:

### 1. calibration curves in ideal SEC:

Provided that the main separation mechanism is exclusively by size, from the classical universal calibration (UC) curve,  $\log M[\eta] = a + bV_e$ , obtained with a set of narrow PS standards of different molecular weights eluted in THF, and taking into account the Mark-Houwink-Sakurada (MHS) equation,  $[\eta] = KM^\alpha$ , a particular calibration for THF-PS can be derived as:

$$\log M = \frac{a - \log K_{PS}}{1 + \alpha_{PS}} + \frac{b}{1 + \alpha_{PS}} V_e \quad (1)$$

where the subscript "PS" refers to the MHS constants for PS in THF at a given temperature.  $M$  will refer to the weight average molar mass.

If the polymer sample is different in chemical nature from PS but is assumed that the UC of the THF-PS reference system is accomplished (i.e., size is the only mechanism accounting for the separation process), the particular calibration curve for the unknown

sample should be:

$$\log M_{UC} = \frac{a - \log K}{1 + \alpha} + \frac{b}{1 + \alpha} V_e \quad (2)$$

with  $K$  and  $\alpha$  being the MHS constants of the solvent-polymer system under elution.

2. calibration curves in SEC with secondary mechanisms:

For polymer samples eluted by a mixture of main (size) and secondary mechanisms, the THF-PS reference calibration is no longer valid.<sup>[21,23,25–32]</sup> In this case, a specific (proper) calibration curve,  $\log M_S[\eta] = a_S + b_S V_e$ , is transformed into:

$$\log M_S = \frac{a_S - \log K}{1 + \alpha} + \frac{b_S}{1 + \alpha} V_e \quad (3)$$

where the subscript “S” refers to any specific sample under study, and  $a_S$  and  $b_S$  are the new fitting parameters. Although this approach is more accurate than assuming the UC of the reference system for sample characterization, it has some drawbacks because a set of narrow standards of the polymer under study are needed to proceed with the calibration, which is not always possible.

3. calibration curves in SEC based on the fractal nature of the gel packing:

The fractal approach<sup>[42]</sup> allows building up a calibration curve for any solvent-polymer system by using only one sample,  $\log M_F[\eta] = a_F + b_F V_e$ . Subscript “F” refers to the fractal method, and  $a_F$  and  $b_F$  are now the corresponding linear fit parameters. Following the same procedure as before, with the aid of the MHS constants, the particular calibration curve of the polymer is given by:

$$\log M_F = \frac{a_F - \log K}{1 + \alpha} + \frac{b_F}{1 + \alpha} V_e \quad (4)$$

The general character of this third method, independent of the gel packing nature, is based on the relationship between the sample elution volume and the overall chromatographic distribution coefficient,  $K_D$ , given by:

$$V_e = V_o + K_D V_p \quad (5)$$

with  $V_o$  and  $V_p$  being the interstitial and pore volumes of the column set, respectively.  $K_D$  represents the ratio of the solute concentration in the stationary and in the mobile phases. This coefficient takes into account, not only the pure exclusion mechanism, but also secondary effects.<sup>[38]</sup> It should be noted that, while the  $M[\eta]$  parameter is exclusively related to the size of the macromolecule (or entropic effects), the  $V_e$  also considers the enthalpic effect due to solvent-polymer-gel interactions. Consequently, it is reasonably expected that the same value of  $M[\eta]$  yield different

values of  $V_e$ , depending on such interactions. Therefore, shifts from the UC curve should be obtained, depending on the chemical nature of the chromatographic system and the gel packing used. In this regard, the crosslinking degree has been related to the entropic contribution to  $V_e$ , whereas the swelling degree was associated with the enthalpic effect.<sup>[24]</sup> Moreover, the coefficient  $K_D$  has also been correlated with the fractal characteristics of the chromatographic support, i.e., the available pore size,  $L$ , and the fractal dimension of the pore surface,  $D_f$ .<sup>[33,34]</sup>

$$K_D = 1 - \left(\frac{R}{L}\right)^{3-D_f} \quad (6)$$

The fractal dimension,  $D_f$ , reflects both the sizes of solutes and their possible solvent-polymer and polymer-gel interactions and, therefore,  $D_f$  should be a better parameter than  $M[\eta]$  for a SEC calibration plot. This fractal parameter is easily calculated for a given solvent-polymer-gel ternary system from experimental elution and viscosity data, by taking natural logarithms in Eq. (6):<sup>[38]</sup>

$$\ln R = \frac{1}{3-D_f} \ln(1-K_D) + \ln L \quad (7)$$

The slope and intercept of the linear plot,  $\ln R$  vs.  $\ln(1-K_D)$ , allow determination of the fractal dimension and the available pore size, respectively, which are characteristic parameters for a given ternary system.  $D_f$  values can be calculated from different ternary systems, and a fractal calibration plot ( $D_f$  vs.  $K_D$ ) can be obtained for a given solute size,<sup>[38]</sup> being both magnitudes simultaneously representative of the entropic and enthalpic effects (or size + interactions) accounting in a SEC chromatographic process.

The procedure to obtain the particular fractal calibration  $\log M_F$  vs.  $V_e$  has been explained in detail elsewhere.<sup>[42]</sup> Briefly, it requires a knowledge of the sample elution profile, the elution volume, the intrinsic viscosity, and the MHS constants,  $K$  and  $\alpha$ , of the system under study. Taking in mind all this information: (a) from  $V_e$  value (the maximum of the chromatogram),  $K_D$  is calculated using Eq. (5); (b) the  $D_f$  value of the specific solvent-polymer system is obtained from the fractal calibration curve; (c) next, the  $L$  value is deduced from Eq. (6) since the viscometric radius  $R$  can be calculated using the Einstein equation,<sup>[38,42]</sup>  $R = 0.5412 (M[\eta])^{1/3}$ ; (d) once the fractal parameters ( $D_f$  and  $L$ ) have been estimated with a unique sample (i.e.,  $M[\eta] = 10^6 \text{ mL} \cdot \text{mol}^{-1}$ ), a relationship between  $V_e$  and  $M[\eta]$  can be obtained by combining Eqs. (5) and (6):

$$V_e = V_o + V_p \left[ 1 - \left( \frac{0.5412(M[\eta])^{1/3}}{L} \right)^{3-D_f} \right] \quad (8)$$

(e) by giving values to  $M[\eta]$  in Eq. (8), the corresponding  $V_e$  elution volumes are obtained and the classical plots  $\log M_F[\eta]$  vs.  $V_e$  or  $\log M_F$  vs.  $V_e$  (Eq. (4)) will be generated.

In each case i), ii), and iii), the chromatogram of the sample is deconvoluted into the corresponding MMD, and  $M_w$  ( $M_w = \sum w_i M_i$ ),  $M_n$  ( $M_n = 1/\sum (w_i/M_i)$ ) and  $I$  ( $I = M_w/M_n$ ) are determined.

## EXPERIMENTAL

### Chemicals

Four different types of polymers have been used: narrow standards of PS from Polymer Standard Service-USA Inc. (Silver Spring, MD) with  $M_w$  given by the supplier (in kDa) of: 4.14, 5.78, 6.87, 17.2, 30, 42, 90.1, 114, 123, 207.9, 355, 400, 657, 1432, 2000, 2700, and 3800. Polybutadiene (PBD) was purchased from Polymer Source Inc. (Dorval, Canada) of  $M_w$  (in kDa): 0.92, 6, 6.25, 34, 42.3, 47, 60.7, 67.3, 87, 94.3, 105.7, 268, 323, 360, and 1120. Poly(dimethylsiloxane) (PDMS) was purchased from Polymer Laboratories (Shropshire, U.K.) and Polymer Source Inc. (Dorval, Canada) of  $M_w$  (in kDa): 1.14, 8.1, 33.5, 41.5, 76, 80.5, 123, 188.4, and 681.6. Poly(methylmethacrylate) (PMMA) was purchased from Polymer Laboratories (Shropshire, U.K.) of  $M_w$  (in kDa): 5.78, 26.9, 70.5, 160.5, 254.7, and 550. The ranges of  $I$  of the used standards were: PS (1.05–1.10), PBD (1.03–1.15), PDMS (1.06–1.23), and PMMA (1.03–1.15).

Tetrahydrofuran (THF), benzene (Bz), toluene (Tol), 1–4 dioxane (Diox), cyclohexane (CHX), hexane (Hex), undecane (UND), hexadecane (HEXD), and methyl ethyl ketone (MEK) of chromatographic grade from Scharlau (Barcelona, Spain) were used as solvents or eluents.

### Viscometric Measurements

The intrinsic viscosity,  $[\eta]$ , of each sample in a given solvent or solvent mixture, at 25°C, was calculated according to the MHS equation. The values of the MHS parameters,  $K$  and  $\alpha$ , for the systems studied are listed in Table 1; they were determined by measuring the specific viscosities as previously described.<sup>[24]</sup>

### Chromatography

A Waters liquid chromatography equipment with a refractive index detector was used for SEC experiments, as described elsewhere.<sup>[43–45]</sup> Columns (each one of 7.8 mm ID  $\times$  300 mm) based on crosslinked PS-DVB

**Table 1.** MHS parameters for different solvent-polymer systems at 25°C

System	$K$ (mLg <sup>-1</sup> )	$\alpha$
THF-PBD	0.0109	0.760
Bz-PBD	0.1120	0.604
Diox-PBD	0.1550	0.541
Bz-PDMS	0.0579	0.572
Tol-PDMS	0.0447	0.601
CHX-PDMS	0.1590	0.534
THF-PS	0.0110	0.725
THF-PMMA	0.0075	0.720
Diox-PMMA	0.0114	0.714
Hex-PDMS	0.0108	0.723
Hex:MEK (80:20)-PDMS	0.0109	0.730
Hex:MEK (60:40)-PDMS	0.0123	0.710
UND:MEK (60:40)-PDMS	0.0247	0.639
UND:MEK (30:70)-PDMS	0.0285	0.611
HEXD:MEK (40:60)-PDMS	0.0579	0.548

copolymer were selected from different suppliers,  $\mu$ -Styragel from Waters (Milford, MA), and TSK Gel H<sub>HR</sub> and TSK Gel H<sub>XL</sub> from Tosohaas, Tosoh Corp. (Tokyo, Japan), and sets of three columns in 'pure' (the same type of column) or mixed combinations were used. Packing characteristics for 'pure' ( $\mu$ -Styragel, TSK Gel H<sub>HR</sub>, TSK Gel H<sub>XL</sub>) and mixed (TSK Gel H<sub>HR-XL-HR</sub>, TSK Gel H<sub>XL-HR-XL</sub>), such as particle size, nominal pore size, interstitial, pore and total exclusion volumes ( $V_o$ ,  $V_p$  and  $V_T$ ), and molar mass separation range are summarized in Table 2.

All solvents used as eluents were previously degassed and filtered by passing them, under vacuum, through a 0.45  $\mu$ m regenerated cellulose filter from Micro Filtration Systems (Dublin, CA). All chromatographic experiments were conducted at 25°C in a thermostated heater, and the columns were equilibrated overnight prior to starting any experiment. Chromatograms were obtained at a flow rate of 1.0 mL · min<sup>-1</sup> by injection of 100  $\mu$ L of sample solution. To avoid concentration effects on the elution volumes, all solute samples were injected at four concentrations and then extrapolated to zero concentration.<sup>[21,46]</sup>

## RESULTS AND DISCUSSION

Figure 1 shows, as an example, universal calibration plots for different binary systems, THF-PS (part A), THF-PBD (part B) and Tol-PDMS (part C), in 'pure'  $\mu$ -styragel, TSK Gel H<sub>HR</sub>, and TSK Gel H<sub>XL</sub> sets. The chemical nature of the polymeric solute was changed, choosing in each case the best



**Table 2.** Column packing characteristics

Commercial name	Gel packing	Pore size	Particle size ( $\mu\text{m}$ )	Effective molar mass range	$V_0$ (mL) <sup>a</sup>	$V_T$ (mL) <sup>b</sup>	$V_P$ (mL)
$\mu$ -Styragel ('pure')	Copolymer PS-DVB	$10^3 \text{ \AA}$ $10^4 \text{ \AA}$ $10^5 \text{ \AA}$	15	200–30000 5000–600000 50000–4 Million	17.70	35.80	18.10
TSK Gel H <sub>HR</sub> ('pure')	Copolymer PS-DVB	G2500 G4000 G6000	5	200–40000 1000–600000 10000–4 Million	16.40	37.40	21.00
TSK Gel H <sub>XL</sub> ('pure')	Copolymer PS-DVB	G2500 G4000 G6000	5 6 9	200–40000 1000–600000 10000–4 Million	17.07	33.70	16.63
TSK Gel H <sub>HR</sub> + H <sub>XL</sub> + H <sub>HR</sub>	Copolymer PS-DVB	G2500 G4000 G6000	5 6 5	200–40000 1000–600000 10000–4 Million	15.83	32.00	16.17
TSK Gel H <sub>XL</sub> + H <sub>HR</sub> + H <sub>XL</sub>	Copolymer PS-DVB	G2500 G4000 G6000	5 5 9	200–40000 1000–600000 10000–4 Million	15.68	31.00	15.32

<sup>a</sup>Determined with a PS standard of high molar mass ( $M = 3\,800\,000$  g/mol).

<sup>b</sup>Determined with small molecules as THF, Tol or Bz;  $V_P = V_T - V_0$ .

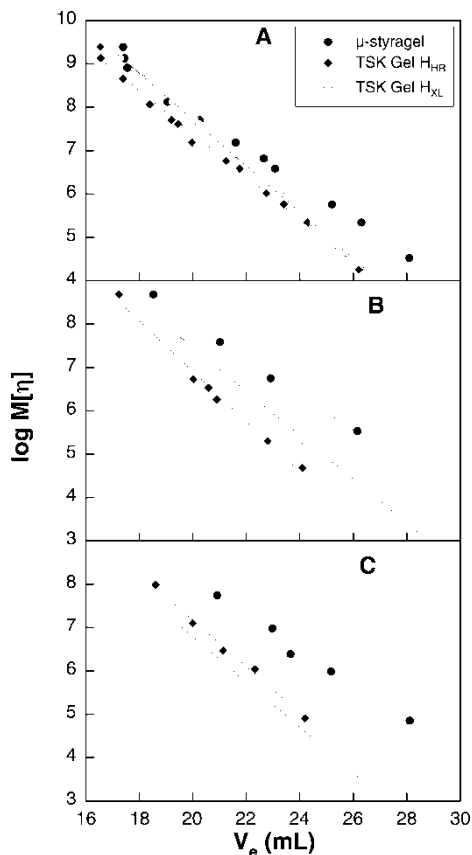


**Figure 1.** Comparison of the elution behaviour at 25°C of the solvent-polymer systems: (A) THF-PS; (B) THF-PBD; and (C) Tol-PDMS, in 'pure' set packings of  $\mu$ -styragel, TSK Gel H<sub>HR</sub>, and TSK Gel H<sub>XL</sub>.

pure solvent for the polymer. The values of the elution volumes,  $V_e$ , were extrapolated to zero concentration ( $c \rightarrow 0$ ) since they are affected by different factors such as the injected solute concentration, the thermodynamic quality of the solvent,<sup>[47,48]</sup> viscous fingering,<sup>[49]</sup> and the preferential sorption.<sup>[50]</sup> among others. Significant deviations from a single UC curve are observed for different solvent-polymer systems in a given gel packing, or even for the same system when eluting in different commercial chromatographic supports. The elution volumes are shifted to lower or higher values than those expected for an ideal size-exclusion separation mechanism, as a consequence of binary interactions between the three components of the system. A given solvent-polymer system elutes differently depending on the gel used, which means that the intrinsic and microscopic nature of the gel is the major responsible of the observed behaviour. Since all the selected

packings are based on a PS-DVB copolymer, the differences in polymer-gel interactions could be mainly attributed to the different gel crosslinking degrees.<sup>[38]</sup> When comparisons of the elution behaviour of a wide variety of solvent-polymer systems were made in a given pure TSK Gel H<sub>XL</sub> column set, as seen in Figure 2, deviations from a unique curve were also observed, mainly due to solvent-gel interactions.

Figure 3 shows the experimental elution behaviour for nine solvent-polymer systems eluted in a mixed TSK Gel H<sub>HR-XL-HR</sub> set. As can be seen, all the systems exhibit linear fits, with  $r \geq 0.997$ , at least in the molar mass range studied here. Shifts from a unique calibration curve are observed, although the deviations were lower than those for 'pure' TSK Gel H<sub>XL</sub> set (Figure 2) or TSK Gel H<sub>HR</sub> set (not shown). As mentioned above, secondary separation mechanisms again appear to be due to polymer-gel or

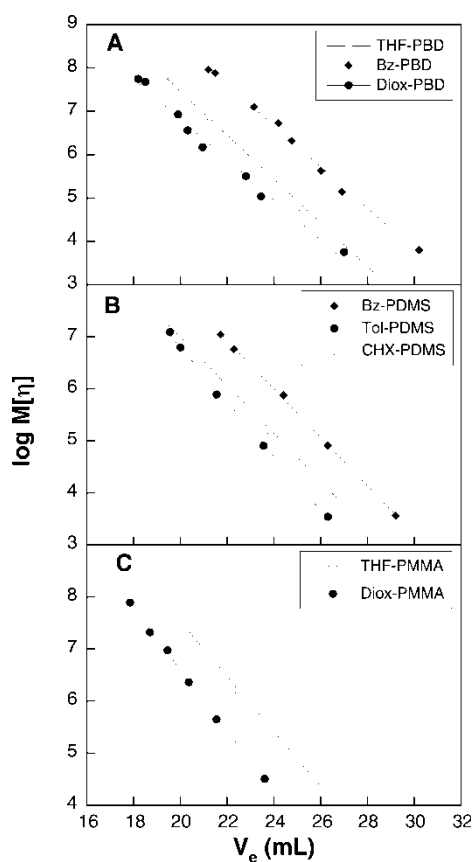


**Figure 2.** Comparison of the elution behaviour at 25°C of different solvent-polymer systems in 'pure' TSK Gel H<sub>XL</sub>, for the following polymeric solutes: (A) PBD; (B) PDMS; and (C) PMMA.

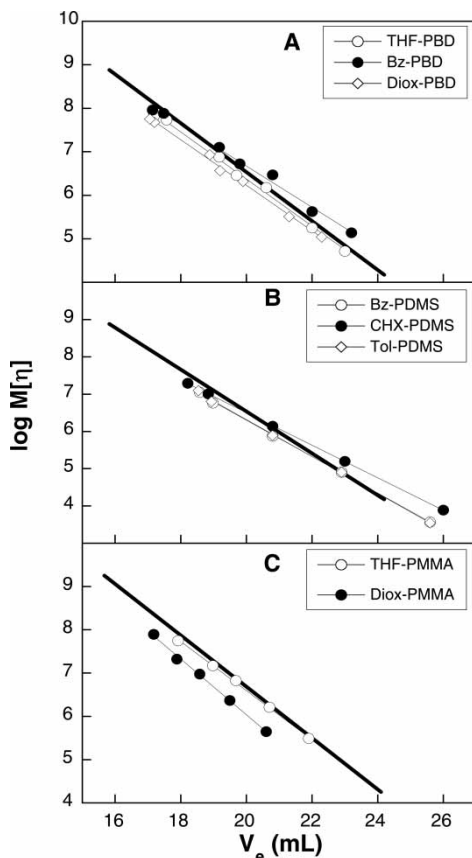


**Figure 3.** Comparison of the elution behaviour at 25°C of different solvent-polymer systems in 'mixed' TSK Gel  $H_{HR+XL+HR}$ , for the following polymeric solutes: (A) PBD; (B) PDMS, and (C) PMMA. The thick line corresponds to the THF-PS reference system.

solvent-gel interactions. If the polymer-gel interactions are attractive, adsorption of the solute onto the packing occurs and the sample elution volume is higher than that according to its size, being its calibration curve placed at the right-hand side of that of the reference THF-PS system. By contrast, earlier elution is observed for systems in which polymer-gel interactions are of a repulsive nature or the attractive solvent-packing interactions predominate. A similar trend is observed for the same systems eluted in the mixed TSK Gel  $H_{XL-HR-XL}$  set and also when using mixed solvents as eluents (not shown).

The above results, shown in Figs. 1–3, indicate that there is not a unique universal calibration curve when plotting  $\log M[\eta]$  (a magnitude that only considers the entropic effects) against the elution volumes (that account for entropic and enthalpic factors) evidencing that solutes are not exclusively

separated by pure or “ideal” SEC. Obviously, the determination of the molar mass for a polymer different from PS using the THF-PS reference curve can lead to important errors as discussed below.

The estimation of the weight average molar masses,  $M_w$ , has been made by deconvoluting the elution profiles (chromatograms) and by transforming them into the classical MMD ( $w_i$  vs.  $V_{e,i}$  or  $w_i$  vs.  $M_i$ ), through the SEC calibration curves given by Eqs. (2), (3), and (4), as previously described.<sup>[42]</sup> In all these calculations, both concentration and axial dispersion effects have not been taken into account. The former effect is not considered because the  $M_w$  values of the samples analyzed were less than 125,000 Da. On the other hand, the influence of the dispersion effects is negligible, given the column dimensions, flow rate, and monodispersities of the samples. The reliability and accuracy of each procedure has been analyzed in terms of the deviations of the  $M_w$  values calculated according to the three methods with respect to the real  $M_w$  value (given by the supplier), denoted as  $M_R$ . These deviations are defined as:<sup>[5,8,42]</sup>

$$dM_X = \frac{|M_X - M_R|}{M_R} \times 100 \quad (9)$$

where  $M_X$  stands for  $M_{UC}$ ,  $M_S$ , or  $M_F$ , that is the molar mass obtained from the chromatographic profile by using Eqs. (2), (3), or (4), respectively.

Tables 3 and 4 summarize, as an example, the values of  $M_{UC}$  and  $dM_{UC}$  (expressed in percentage) obtained for several polymers in pure or mixed solvents using different column sets. As can be seen, the  $M_{UC}$  values estimated by the procedure that assumes the THF-PS universal system as reference (Eq. (2)) differ considerably from the  $M_R$  values given by the suppliers. In fact, an overall mean deviation of about 93% in the molar mass has been estimated, which indicates that (in practice) the classical universal procedure is poorly accomplished by any solvent-polymer system since, in addition to size, other separation mechanisms are present. In order to establish the degree of confidence in the determination of molar masses, it is necessary to assume a new calibration curve made-up with standards of the same chemical nature as the polymeric sample under characterization, which is usually different enough to the THF-PS one (see Figs. 1–3). The values of  $M_S$  evaluated by transforming the chromatograms according to Eq. (3) (i.e., with the new calibration curve as reference) are also included in Tables 3 and 4. The corresponding linear fit coefficients needed for calculations (named  $a_S$  and  $b_S$ ) are compiled in Table 5. Overall, for any solvent-polymer system, the deviations  $dM_S$  were considerably lower (with a mean value of about 13%) than those obtained with the THF-PS curve in all sets of columns assayed. These results provide quantitative evidence for the importance of using a proper (specific) calibration curve for each polymeric system analyzed. However, from a practical point of view, it can be very difficult (if not impossible) to obtain a broad set of narrow standards (tailor-made) for a given polymer sample. This can be a reason for the wide use of

**Table 3.** Molar masses,  $M_{UC}$ ,  $M_S$  and  $M_F$  calculated with Eqs. (2), (3), and (4), respectively, and their respective deviations (in %) estimated with Eq. (9) respect to the molar masses given by the supplier,  $M_R$ , for ‘pure’ TSK Gel H<sub>HR</sub> and ‘pure’ TSK Gel H<sub>XL</sub> set packings

Packing	System	$M_R$	$M_{UC}$	$dM_{UC}$ (%)	$M_S$	$dM_S$ (%)	$M_F$	$dM_F$ (%)
TSK Gel H <sub>HR</sub>	THF-PBD	67 300	140 600	108.9	74 200	10.2	62 800	6.7
	Bz-PBD	47 000	43 500	7.4	39 500	15.9	33 600	28.5
	Diox-PBD	67 300	50 700	24.7	68 500	1.8	57 300	14.9
	Bz-PDMS	41 470	39 800	4.0	43 000	3.7	41 300	0.4
	Tol-PDMS	41 470	65 000	56.7	42 500	2.5	44 800	8.0
	CHX-PDMS	76 035	45 300	40.4	86 100	13.2	67 000	11.9
TSK Gel H <sub>XL</sub>	THF-PBD	34 000	48 200	41.8	38 000	11.8	31 100	8.5
	Bz-PBD	12 600	2 600	79.4	14 400	14.3	13 900	10.3
	Bz-PDMS	33 500	19 100	43.0	35 300	5.4	33 300	0.6
	Tol-PDMS	8 100	31 900	293.8	8 900	9.9	5 900	27.2
	Tol-PDMS	33 500	166 200	396.1	45 700	36.4	38 500	14.9

Intercepts ( $a_x$ ) and slopes ( $b_x$ ) from calibration curves, needed for calculations, were taken from ref. [42].

**Table 4.** Molar masses,  $M_{UC}$ ,  $M_S$  and  $M_F$  calculated with Eqs. (2), (3), and (4), respectively, and their respective deviations (in %) estimated with Eq. (9) respect to the molar masses given by the supplier,  $M_R$ , for TSK Gel H<sub>HR-XL-HR</sub> and ‘pure’  $\mu$ -styragel set packings

Packing	System	$M_R$	$M_{UC}$	$dM_{UC}$ (%)	$M_S$	$dM_S$ (%)	$M_F$	$dM_F$ (%)
TSK Gel H <sub>HR-XL-HR</sub>	THF-PBD	12 600	15 250	17.4	13 040	3.4	13 520	6.8
	Bz-PBD	42 300	24 440	73.1	32 840	28.8	37 440	13.0
	Diox-PBD	60 700	99 030	38.7	60 410	24.1	46 950	29.3
	Bz-PDMS	33 500	52 070	35.6	39 280	14.7	35 950	6.8
	Bz-PDMS	123 000	186 390	34.0	117 650	4.6	116 160	5.9
$\mu$ -styragel	Tol-PDMS	33 500	51 370	34.8	39 460	15.1	36 550	8.3
	Hex-PDMS	33 500	38 360	14.5	37 810	12.8	31 520	5.9
	Hex:MEK(80:20)-PDMS	33 500	40 820	21.8	38 040	13.5	33 680	0.5
	Hex:MEK(60:40)-PDMS	33 500	57 200	70.7	38 790	15.7	33 070	1.3
	UND:MEK(60:40)-PDMS	80 500	146 040	81.4	97 960	7.6	71 180	11.6
	UND:MEK(30:70)-PDMS	80 500	150 750	87.2	99 130	23.1	85 260	5.9
	HEXD:MEK(40:60)-PDMS	80 500	180 040	123.6	94 700	17.6	93 810	16.5

**Table 5.** Linear fit coefficients of different systems eluted in TSK Gel H<sub>HR-XL-HR</sub> and ‘pure’  $\mu$ -styragel set packings

Packing	System	$a_S$	$b_S$ (mL <sup>-1</sup> )	$a_F$	$b_F$ (mL <sup>-1</sup> )
TSK Gel H <sub>HR-XL-HR</sub>	THF-PBD	17.20	-0.541	13.44	-0.367
	Bz-PBD	16.16	-0.474	18.19	-0.567
	Diox-PBD	16.69	-0.523	24.08	-0.915
	Bz-PDMS	16.08	-0.489	16.65	-0.519
	Tol-PDMS	16.22	-0.495	16.70	-0.521
$\mu$ -styragel	Hex-PDMS	15.14	-0.372	14.61	-0.356
	Hex:MEK(80:20)-PDMS	15.77	-0.400	15.04	-0.373
	Hex:MEK(60:40)-PDMS	15.82	-0.412	15.27	-0.394
	UND:MEK(60:40)-PDMS	16.39	-0.438	18.74	-0.552
	UND:MEK(30:70)-PDMS	15.51	-0.398	19.00	-0.560
	HEXD:MEK(40:60)-PDMS	13.79	-0.327	19.10	-0.566

Data for UC are obtained from the linear fit of the THF-PS reference system eluted in both sets, being:  $a = 17.78$  and  $b = -0.562$  mL<sup>-1</sup> for TSK Gel H<sub>HR-XL-HR</sub> and  $a = 15.91$  and  $b = -0.403$  mL<sup>-1</sup> for ‘pure’  $\mu$ -styragel.

PS standards in THF or other solvents, and the so-called universal calibration curve for polymer characterization.

The errors in the estimation of molar masses can greatly decrease by using the FC approach. In this regard, it should be taken in mind that entropic and enthalpic effects are intimately related to the crosslinking and swelling degrees, respectively, of the chromatographic support.<sup>[24]</sup> Both packing characteristics can be described by the fractal surface that the polymeric solute “encounters” when permeating into the pores of the gel. The fractality of the surface is usually represented by the fractal dimension,  $D_f$ , and both  $D_f$  and  $V_e$  are magnitudes representative of the entropic and enthalpic aspects of the chromatographic separation process.<sup>[51]</sup> The evaluation of  $D_f$  and the available pore size,  $L$ , can be made from the slopes and intercepts, respectively, of the linear fits of Eq. (7). As an example, data of  $D_f$  and  $L$  obtained for different systems, at  $V_h = 10^6$  mL · mol<sup>-1</sup>, are compiled in Table 6, together with the values of the distribution coefficient  $K_D$ . As seen, there is a  $D_f$  value for each system independently of the molar mass of the polymeric solute, since the fractal dimension is a parameter characteristic of the pore surface as swollen by the solvent. The fractal dimension,  $D_f$ , ranges between 2.6 and 2.9 for the columns assayed, that is, near the upper limit of 3 (three-dimensional surface), which denotes a high separation efficiency of these supports. In fact, as seen in Figure 4, a linear relationship has been found between  $K_D$  and  $D_f$  for a given solute size (i.e.,  $M[\eta] = V_h = 10^6$  mL · mol<sup>-1</sup>) given by:

$$D_f = 3.036 - 0.792 K_D \quad (10)$$



**Table 6.** Chromatographic distribution coefficients,  $K_D$ , and fractal properties,  $D_f$  and  $L$ , for different polymeric gel packings (data for  $V_h = M[\eta] = 10^6 \text{ mL} \cdot \text{mol}^{-1}$ )

System	$\mu$ -styragel			TSK Gel H <sub>HR</sub>			TSK Gel H <sub>XL</sub>		
	$K_D$	$D_f$	$L$ (Å)	$K_D$	$D_f$	$L$ (Å)	$K_D$	$D_f$	$L$ (Å)
THF-PBD	0.405	2.73	403	0.246	2.86	446	0.350	2.79	420
Bz-PBD	0.521	2.63	428	0.302	2.84	507	0.501	2.72	686
Diox-PBD	0.659	2.49	509	0.317	2.84	648	0.282	2.80	278
Bz-PDMS	0.434	2.66	317	0.313	2.81	430	0.416	2.70	356
Tol-PDMS	0.427	2.71	400	0.275	2.84	455	0.267	2.80	266
CHX-PDMS	0.463	2.67	395	0.353	2.80	513	0.305	2.77	273
THF-PS	0.379	2.74	408	0.307	2.83	528	0.370	2.78	497
THF-PMMA							0.350	2.77	375
Diox-PMMA							0.238	2.83	276

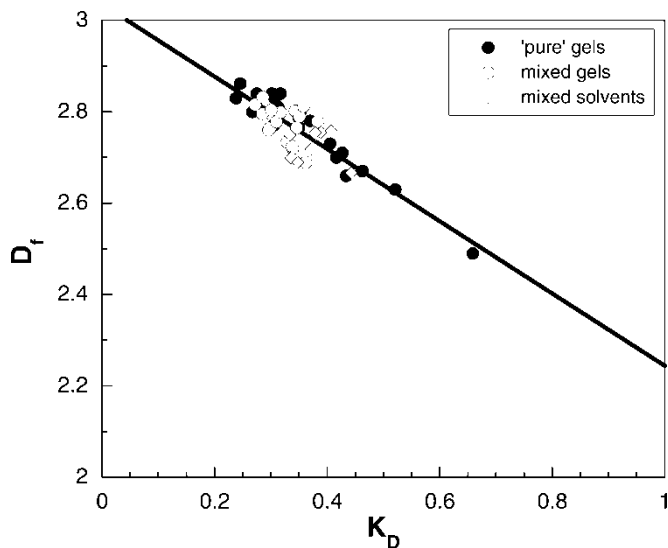


**Figure 4.** Fractal calibration plot for all the systems eluted in: (●) 'pure'  $\mu$ -styrigel, TSK Gel H<sub>HR</sub> and TSK Gel H<sub>XL</sub>; (○) mixed TSK Gel H<sub>HR+XL+HR</sub> and TSK Gel H<sub>XL+HR+XL</sub> columns and (◇) mixed solvents at  $V_h = 10^6 \text{ mL} \cdot \text{mol}^{-1}$ .

This equation represents, already, a universal fractal calibration, since it is fulfilled by many different solvent-polymer-gel systems and provides a tool to characterize an unknown sample. A similar linearity was found for other different values of  $V_h$  not shown here for simplicity.

At this time, according to the procedure indicated previously (Theory section, part iii)), a particular fractal calibration curve can be generated in order to determine average molar masses. The values of  $M_F$  estimated from the chromatographic profile and Eq. (4) are also compiled in Tables 3 and 4 for the different systems assayed. In general, it can be observed that, for a given solvent-polymer-gel system, the deviations relative to the values from the manufacturer, referred as  $dM_F$ , are noticeably lower than those estimated from the classical universal calibration ( $dM_{UC}$ ). The mean percentage deviation found with the FC procedure, for all the 47 ternary systems studied, is of 17% and quite similar to the estimated from the specific calibration curve, 15%, but impressively lower than that from de THF-PS curve, 62%.

Figure 5 shows, as an example, the overlays of the MMD (as  $w_i$  vs.  $M_i$ ) obtained with the three calibration approaches here compared, Eqs. (2), (3), and (4). Part A of the figure corresponds to PBD of  $M_w = 12600 \text{ Da}$  eluted with Bz in TSK Gel H<sub>XL</sub>, and part B for PBD of  $M_w = 67300 \text{ Da}$ , eluted with THF in TSK Gel H<sub>HR</sub>. As can be seen, the MMDs obtained with the fractal calibration approach (Eq. (4)) are nearly overlapping the real MMDs of the samples (Eq. (3)), whereas the ones obtained with the classical THF-PS universal calibration (Eq. (2)) are further apart. Moreover, it is important

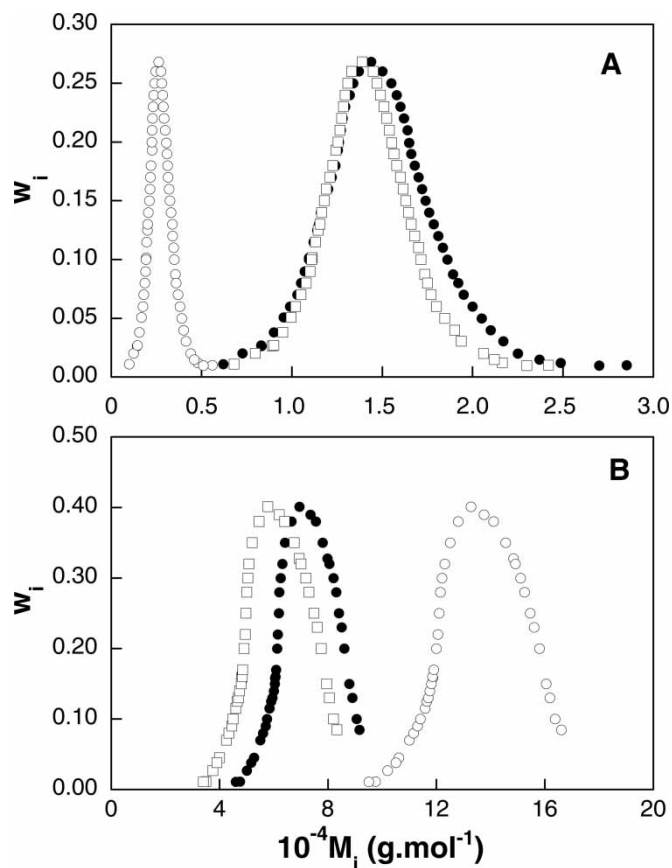


**Figure 5.** Molar mass distributions obtained from the deconvolution with (○) Eq. (2), (●) Eq. (3) and (□) Eq. (4) of the elution profiles of: (A) PBD ( $M_w = 12\,600$ ) in Bz-TSK Gel H<sub>XL</sub> and (B) PBD ( $M_w = 67\,300$ ) in THF-TSK Gel H<sub>HR</sub>.

to note that not a fundamental difference in the shape of the MMDs is observed given that the three equations, used to transform the elution profiles into a MMD, have the same mathematical functionality. However, substantial shifts along the molar mass values are observed, which lead to important errors (as shown in Tables 3 and 4) when determining the molar mass of a sample. Similar plots have been built up for all the systems and columns assayed and have shown the same trend as that observed for the selected examples.

Finally, Figure 6 depicts, as an example, calibration plots (as  $\log M_w$  vs.  $V_e$ ) obtained at 25°C for the THF-PBD system eluted in TSK Gel H<sub>HR</sub> columns (part A) and Bz-PBD system in TSK Gel H<sub>XL</sub> columns (part B), in order to graphically visualize and compare the three calibration methods in the complete  $M_w$  range assayed. Again, and in both sets of columns, the

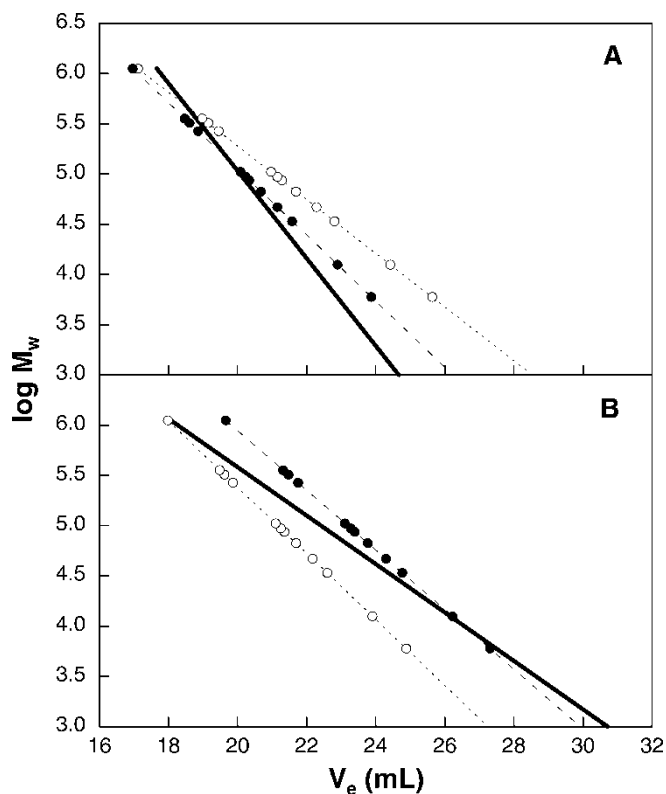


**Figure 6.** Calibration curves at 25°C fitted according to (○) Eq. (2), (●) Eq. (3) and (—) generated from Eq. (4) for the systems: (A) THF-PBD-TSK Gel H<sub>HR</sub> and (B) Bz-PBD-TSK Gel H<sub>XL</sub>.

fractal calibration curves are near to the specific curves, whereas the universal calibration dependence is shifted apart, denoting that parallel to size-exclusion, enthalpic mechanisms also govern the chromatographic separation. Similar trends have been observed for the remaining solvent-polymer-gel systems analyzed. As recently stated,<sup>[9]</sup> the validity of the UC curve should be confirmed prior to its use, for each particular chromatographic system, in order to avoid unacceptable errors. However, the alternative dedicated calibration can be a tedious and time-consuming task and even impracticable in the absence of proper standards. Consequently, the fractal calibration emerges as a valuable tool to determine  $M_w$  values with a similar accuracy. Obviously, from the values of the weight-average molar masses, the corresponding  $M_n$  and polydispersity index can be derived, in order to complete the polymer characterization by SEC. Finally, it should be also emphasized that, when using the fractal calibration, the  $M[\eta]$  value of the particular sample is not a drawback, since a fractal calibration equation (similar to

Eq. (10) can be generated for any  $M[\eta]$  value. In this sense, work is in progress in our lab to extend and generalize the formalism to any hydrodynamic size.

## ACKNOWLEDGMENTS

Financial support from Dirección General de Enseñanza Superior of Spanish MEC (Project MAT 2003-00668) and to Generalitat Valenciana (Project GV 2004-B-133 and Grupos 2004-26) is gratefully acknowledged.

## REFERENCES

1. Lou, X.; van Dongen, J.L.J.; Meijer, E.W. Off-line size-exclusion chromatographic fractionation-matrix-assisted laser desorption ionization time-of-flight mass spectrometry. Theoretical and experimental study. *J. Chromatogr. A* **2000**, *896* (1–2), 19–30.
2. Netopilík, M. Influence of peak-broadening and interdetector volume error on size-exclusive chromatographic analysis with dual viscometric-concentration detection using the universal calibration method. *J. Chromatogr. A* **2001**, *915* (1–2), 15–24.
3. Netopilík, M.; Podzimek, S.; Kratochvíl, P. Estimation of width of narrow molecular weight distributions by size exclusion chromatography with concentration and light scattering detection. *J. Chromatogr. A* **2001**, *922* (1–2), 25–36.
4. Van der Heyden, Y.; Popovici, S.T.; Shoenmakers, P.J. Evaluation of size-exclusion chromatography and size-exclusion electrochromatography calibration curves. *J. Chromatogr. A* **2002**, *957* (2), 127–137.
5. Nassivera, T.; Eklund, A.G.; Landry, C.C. Size-exclusion chromatography of low-molecular-mass polymers using mesoporous silica. *J. Chromatogr. A* **2002**, *973* (1–2), 97–101.
6. Shi Song, M.; Xian Hu, G.; Yu Li, X.; Zhao, B. Study on the concentration effects in size exclusion chromatography. VII. A quantitative verification for the model theory of concentration and molecular mass dependences of hydrodynamic volumes for polydisperse polymers. *J. Chromatogr. A* **2002**, *961* (2), 155–170.
7. Chaidedgumjorn, A.; Suzuki, A.; Toyoda, H.; Toida, T.; Imanari, T.; Linhardt, R.J. Conductivity detection for molecular mass estimation of per-O-sulfonated glycosaminoglycans separated by high-performance size-exclusion. *J. Chromatogr. A* **2002**, *959* (1–2), 95–102.
8. Kaur, M.; Jumel, K.; Hardie, K.R.; Hardman, A.; Meadows, J.; Melia, C.D. Determining the molar mass of a plasma substitute succinylated gelatin by size exclusion chromatography-multi-angle laser light scattering, sedimentation equilibrium and conventional size exclusion chromatography. *J. Chromatogr. A* **2002**, *957* (2), 139–148.
9. Strlic, M.; Kolenc, J.; Kolar, J.; Pihlar, B. Enthalpic interactions in size exclusion chromatography of pullulan and cellulose in LiCl-N,N-dimethylacetamide. *J. Chromatogr. A* **2002**, *964* (1–2), 47–54.
10. Ding, F.; Stol, R.; Kok, W.T.; Poppe, H. Determination of the molecular mass distribution of synthetic polymers by size-exclusion electrochromatography. *J. Chromatogr. A* **2001**, *924* (1–2), 239–249.

11. Yau, W.W.; Kirkland, J.J.; Bly, D.D. Modern size-exclusion liquid chromatography. In *Practice of Gel Permeation and Gel Filtration Chromatography*; Wiley: New York, 1979.
12. Mori, S.; Marechal, H.; Suzuki, H. Evaluation of "solvent-peak separation" column for the determination of polymer molecular mass averages by SEC. *Intl. J. Polym. Anal. Charact.* **1998**, *4* (2), 87–98.
13. Oliva, A.; Llabrés, M.; Fariña, J.B. Comparative study of protein molecular weights by size-exclusion chromatography and laser-light scattering. *J. Pharm. Biomed. Anal.* **2001**, *25* (5–6), 833–841.
14. Campos, A.; Soria, V.; Figueruelo, J.E. Polymer retention mechanism in GPC on active gels, 1: polystyrene in pure and mixed eluents. *Makromol. Chem.* **1979**, *180* (8), 1961–1974.
15. Figueruelo, J.E.; Soria, V.; Campos, A. Polymer retention mechanisms in GPC on active gels, 3. Poly(dimethylsiloxane) and poly(methyl methacrylate). *Makromol. Chem.* **1981**, *182* (5), 1525–1532.
16. Striegel, A.M.; Timpa, J.D.; In *Strategies in Size Exclusion Chromatography*; Potschka, M. and Dubin, P.L., (eds.); American Chemical Society: Washington DC, 1996, Vol. 635, 366–378.
17. Striegel, A.M.; Timpa, J.D. Gel Permeation Chromatography of polysaccharides using universal calibration. *Intl. J. Polym. Anal. Charact.* **1996**, *2*, 213–220.
18. Ciecanska, D.; Strobin, G.; Boryniec, S.; Struszczyk, H. Biotransformation of cellulose: GPC studies. *Intl. J. Polym. Anal. Charact.* **1998**, *4* (3), 205–217.
19. Janco, M.; Berek, D.; Prudskova, T. Liquid-chromatography of polymer mixtures applying a combination of exclusion and full adsorption mechanisms. 2. eluent switching approach. *Polymer* **1995**, *36* (17), 3295–3299.
20. Skvortsov, A.M.; Gorbunov, A.A.; Berek, D.; Trathnigg, B. Liquid chromatography of macromolecules at the critical adsorption point: behaviour of a polymer chain inside pores. *Polymer* **1998**, *39* (2), 423–429.
21. Berek, D. Interactive properties of polystyrene/divinylbenzene based commercial SEC columns. In *Column Handbook for Size Exclusion Chromatography*; Wu, C., (ed.); Academic Press: San Diego, CA, 1999, 445–457.
22. Gómez, C.M.; García, R.; Figueruelo, J.E.; Campos, A. Theoretical evaluation of  $K_p$  in size-exclusion chromatography from a thermodynamic viewpoint. *Macromol. Chem. Phys.* **2000**, *201* (17), 2354–2364.
23. García, R.; Gómez, C.M.; Figueruelo, J.E.; Campos, A. Thermodynamic interpretation of the SEC behavior of polymers in a polystyrene gel matrix. *Macromol. Chem. Phys.* **2001**, *202* (9), 1889–1901.
24. García, R.; Recalde, I.B.; Figueruelo, J.E.; Campos, A. Quantitative evaluation of the swelling and crosslinking degrees in two organic gels packings for SEC. *Macromol. Chem. Phys.* **2001**, *202* (17), 3352–3362.
25. Belenkii, B.G.; Vilenchick, L.Z. *Modern Liquid Chromatography of Macromolecules*; Elsevier: Amsterdam, 1983; 105–114.
26. García, R.; Porcar, I.; Campos, A.; Soria, V.; Figueruelo, J.E. Solution properties of polyelectrolytes. VIII. A comparative study of the elution behaviour between two organic-based packings. *J. Chromatogr. A* **1993**, *655* (2), 191–198.
27. Campos, A.; García, R.; Porcar, I.; Soria, V. Solution properties of polyelectrolytes. XI. Adsorption effects in aqueous size-exclusion chromatography of polyanions. *J. Liq. Chromatogr.* **1994**, *17* (14–15), 3261–3283.
28. Shah, G.; Dubin, P.L. Adsorptive interaction of Ficoll standards with porous glass size-exclusion chromatography columns. *J. Chromatogr. A* **1995**, *693* (2), 197–203.

29. García, R.; Porcar, I.; Figueruelo, J.E.; Soria, V.; Campos, A. Solution properties of polyelectrolytes. XII. Semi-quantitative approach to mixed electrostatic and hydrophobic polymer-gel interactions. *J. Chromatogr. A* **1996**, *721* (2), 203–212.
30. Berek, D.; Janco, M.; Meira, G.R. Liquid chromatography of macromolecules at the critical adsorption point. II. Role of column packing: bare silica gel. *J. Polym. Sci. Part A: Polym. Chem.* **1998**, *36* (9), 1363–1371.
31. Kosmas, M.K.; Bokaris, E.P.; Georgaka, E.G. The effects of substrate interactions in the liquid chromatography of polymers. *Polymer* **1998**, *39* (20), 4973–4976.
32. Mori, S.; Barth, H.G. *Size Exclusion Chromatography*; Springer, Berlin, 1999; 11–23.
33. Brochard, F. Some surface effects in porous fractals. *J. Phys.* **1985**, *46*, 2117–2123.
34. Brochard, F.; Ghazi, A.; le Maire, M.; Martin, M. Size exclusion chromatography on porous fractals. *Chromatographia* **1989**, *27*, 257–263.
35. Eisenriegler, E. *Polymers Near Surfaces*; World Scientific: Singapore, 1993.
36. Fleer, G.J. *Polymers at Interfaces*; Chapman & Hall: London, 1993.
37. Garel, T.; Orland, H. Directed polymers in a random medium: a variation approach. *Phys. Rev. B* **1997**, *55* (1), 226–230.
38. García-Lopera, R.; Irurzun, I.; Abad, C.; Campos, A. Fractal calibration in size-exclusion chromatography. I. An introduction. *J. Chromatogr. A* **2003**, *996* (1–2), 33–43.
39. Huber, G.; Vilgis, T.A. Polymer adsorption on heterogeneous surfaces. *Eur. Phys. J. B* **1998**, *3* (2), 217–223.
40. Guillaume, Y.C.; Robert, J.F.; Guinchart, C. A mathematical model for hydrodynamic and size exclusion chromatography of polymers on porous particles. *Anal. Chem.* **2001**, *73* (13), 3059–3064.
41. Duca, D.; Deganello, G. Analysis by size exclusion chromatography (SEC) of catalytic materials: the fractal properties and the pore size distribution of pumice. *J. Mol. Catal. A-Chem.* **1996**, *112* (3), 413–421.
42. García-Lopera, R.; Codoñer, A.; Bañó, M.C.; Abad, C.; Campos, A. Size-exclusion chromatographic determination of polymer molar mass averages using a fractal calibration. *J. Chromatogr. Sci.* **2005**, *43* (5), 226–234.
43. García, R.; Celda, B.; Soria, V.; Tejero, R.; Campos, A. Non-exclusion phenomena in SEC with inorganic porous packing. A thermodynamic treatment. *Polymer* **1990**, *31* (9), 1694–1702.
44. García-Lopera, R.; Gómez, C.M.; Falo, M.; Abad, C.; Campos, A. Chromatographic evaluation of resolution and secondary mechanisms of pure and mixed sets of columns: TSK gel H<sub>HR</sub> and TSK gel H<sub>XL</sub>. *Chromatographia* **2004**, *59* (5/6), 355–360.
45. Campos, A.; Gómez, C.M.; García, R.; Figueruelo, J.E.; Soria, V. Extension of the Flory-Huggins theory to study incompatible polymer blends in solution from phase separation data. *Polymer* **1996**, *37* (15), 3361–3372.
46. Gómez, C.M.; Figueruelo, J.E.; Campos, A. Evaluation of thermodynamic parameters for blends of polyether sulfone and poly(methylmethacrylate) or polystyrene in dimethylformamide. *Polymer* **1998**, *39* (17), 4023–4032.
47. Campos, A.; Borque, L.; Figueruelo, J.E. Selection of optimum conditions for use of microstyragel columns. *Anal. Quím.* **1978**, *74* (5), 701–707.
48. Figueruelo, J.E.; Campos, A.; Soria, V.; Tejero, R. A model accounting for concentration effects in exclusion chromatography. *J. Liq. Chromatogr.* **1984**, *7* (6), 1061–1078.
49. Janca, J. Concentration effects in gel-permeation chromatography I. Polymer-solution properties. *J. Chromatogr.* **1977**, *134* (2), 263–272.

50. García-Lopera, R.; Gómez, C.M.; Abad, C.; Campos, A. An analysis of the concentration effects on elution volumes by using the preferential solvation parameter in two SEC packings. *Macromol. Chem. Phys.* **2002**, *203* (18), 2551–2559.
51. Porcar, I.; García, R.; Soria, V.; Campos, A.; Figueruelo, J.E. Porous fractal gels: secondary effects in SEC. *J. Non-Crystall. Sol.* **1992**, *147&148*, 170–175.

Received January 16, 2007

Accepted February 12, 2007

Manuscript 6033